ACS Catalysis

Research Article

pubs.acs.org/acscatalysis

Bioinspired Approach to Multienzyme Cascade System Construction for Efficient Carbon Dioxide Reduction

Xiaoli Wang,[†,‡,§] Zheng Li,[†,§] Jiafu Shi,[†,§] Hong Wu,[†,§] Zhongyi Jiang,*[†,‡,§] Wenyan Zhang,[†,§] Xiaokai Song,[†,§] and Qinghong Ai[†,§]

[†]Key Laboratory for Green Chemical Technology of Ministry of Education, School of Chemical Engineering and Technology, Tianjin University, Tianjin 300072, P. R. China

[‡]National Key Laboratory of Biochemical Engineering, Institute of Process Engineering, Chinese Academy of Sciences, Beijing 100190, P. R. China

[§]Collaborative Innovation Center of Chemical Science and Engineering (Tianjin), Tianjin 300072, P. R. China

Supporting Information

ABSTRACT: An efficient multienzyme cascade system based on ultrathin, hybrid microcapsules was constructed for converting CO_2 to methanol by combining the unique functions of catechol and gelatin. Gelatin was modified with catechol groups (GelC) via well-defined EDC/NHS chemistry, thus endowed with the ability to covalently attach enzyme molecules. Next, the first enzyme (FateDH)-containing $CaCO_3$ templates were synthesized via coprecipitation and coated with a GelC layer. Afterward, GelC was covalently attached with the second enzyme (FaldDH) via Michael addition and Schiff base reactions. Then, GelC induced the hydrolysis and condensation of silicate, and the third enzyme (YADH) was entrapped accompanying the formation of silica particles. After removal of $CaCO_3$ templates, the GelCSi-based multienzyme system was obtained, in which the three enzymes were appropriately positioned in different places of the GelCSi microcapsules, and the amount of individual enzyme was regulated according to enzyme activity. The system exhibited high activity and stability for converting CO_2 into methanol. In detail, the system displayed much higher methanol yield and selectivity (71.6%, 86.7%) than that of multienzyme in free form (35.5%, 47.3%). The methanol yield remained 52.6% after nine times of recycling. This study will provide some guidance on constructing diverse scaffolds for applications in catalysis, drug and gene delivery, and biosensors.

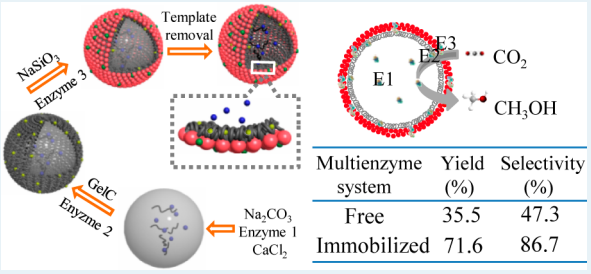

Multienzyme system	Yield (%)	Selectivity (%)
Free	35.5	47.3
Immobilized	71.6	86.7

KEYWORDS: *CO_2 conversion, multienzyme cascade system, mussel-inspired chemistry, biomimetic mineralization, hybrid microcapsules*

1. INTRODUCTION

Owing to the increasing energy and environmental pressures, utilization of CO_2 as a raw material for the synthesis of commodity chemicals and fuels seems to be a promising solution to mitigate the gradual increase in atmospheric CO_2 content. The predominant methods for CO_2 utilization encompass chemical conversion, biological conversion, and enzymatic conversion in vitro.[1−5] In comparison, enzymatic conversion seems to be a particularly competitive method due to its intrinsic merits such as high yield and selectivity under milder and greener reaction conditions.[4,6−8]

A multienzyme-based approach for CO_2 conversion, utilizing naturally occurring reactions, may prove efficient and cost-effective,[9−11]although CO_2 is so thermodynamically and kinetically stable that it rarely uses its fullest potential. However, the enzyme in free form is liable and cannot be easily recovered for long-term reuse, and consequently, it cannot meet the requirements for industrial applications.[12−14] Thus, it is imperative to rationally design immobilization scaffolds and protocols for a stable and recyclable multienzyme system. Dave et al. utilized three different dehydrogenases which were coimmobilized in silica matrices to convert CO_2 to methanol.[15] Soon after, Wang et al. used the polystyrene particles to coimmobilize the three different dehydrogenases and glutamate dehydrogenases for the production of methanol from CO_2 with in situ cofactor regeneration.[16] Although these methods were proven successfully, the enzyme dosage per batch of these methods was usually large, because the amount of individual enzyme cannot be flexibly regulated, and the time to reach reaction equilibrium was usually long because of high mass transfer resistance. In our previous studies, spatially separated enzymatic systems, mimicking natural enzyme organization, were developed by using several kinds of organic−inorganic hybrid microcapsules.[17−21] To sum up, a desirable multienzyme system may bear the following features: (1) enabling the expedient regulation of the amount of

Received: November 21, 2013
Revised: February 4, 2014
Published: February 12, 2014

individual enzyme according to enzyme activity; (2) enabling the ordered assembly of enzymes within nanometer distances to facilitate substrate channeling and the direct transfer of an intermediate between consecutive enzymes without equilibrating with the bulk fluid; (3) enabling the fine adjustment of pore size of the scaffold to acquire low mass transfer resistance for the intermediates/products; (4) enabling the easy recovery and recycling of immobilized enzyme. Therefore, designing a novel and high-efficiency immobilization scaffold and protocol for robust and recyclable multienzyme system would be of great significance.

Mussel-inspired chemistry has been proved as a powerful and versatile paradigm to create tailored structures with desirable properties in a more facile way.[22−25] Catechol is the side chain of 3,4-dihydroxy-L-phenylalanine (DOPA), abundantly present in mussel-adhesive proteins. Catechol-modified polymers including alginate, hyaluronic acid, chitosan, and poly(ethylene glycol) have been used to prepare microcapsules,[26] hydrogel,[27−29] and coatings.[30,31] Especially, molecules containing catechol groups were able to react with the amine-containing molecules through Michael addition and Schiff base reactions.[32,33] Recently, various biomolecules have been immobilized with the aid of catechol-containing polymers, and the bioactivity of biomolecules was well retained.[33−36]

The aim of the present study was to fabricate ultrathin, hybrid microcapsules for constructing a multienzyme cascade system to efficiently convert CO_2 into methanol. First, gelatin was modified by catechol groups using EDC/NHS as amine coupling agents, thus endowed with the ability to covalently attach enzyme molecules. Afterward, the catechol-modified gelatin (GelC) was deposited onto $CaCO_3$ templates to form the GelC layer. Subsequently, GelC induced the hydrolysis and condensation of silicate precursor to silica nanoparticles,[37,38] generating the mesoporous silica layer as the shell of the microcapsules. Three enzymes, formate dehydrogenase (FateDH, enzyme 1), formaldehyde dehydrogenase (FaldDH, enzyme 2), and alcohol dehydrogenase (YADH, enzyme 3), were respectively immobilized through physical entrapment in the microcapsule lumen, covalent attachment onto the GelC layer, and physical entrapment in the silica layer. The resultant multienzyme system acted as an enzymatic microfactory to consecutively convert carbon dioxide (CO_2) into methanol.

2. EXPERIMENTAL SECTION

2.1. Materials. Formate dehydrogenase from *Candida boidinii* (FateDH, EC.1.2.1.2, F8649), formaldehyde dehydrogenase from *Pseudomonas* sp. (FaldDH, EC.1.2.1.46, F1879), yeast alcohol dehydrogenase (YADH, EC 1.1.1.1, A7011), reduced nicotinamide adenine dinucleotide (NADH, 98 wt %), poly(allylamine hydrochloride) (PAH, MW ∼15 000), gelatin (Type B from bovine skin, ∼225 bloom, and type A from porcine skin, >300 bloom), fluorescein isothiocyanate (FITC), tris(hydroxymethyl)amiomethane (Tris), and poly(sodium 4-styrenesulfonate) (PSS, MW ∼70 000) were purchased from Sigma-Aldrich Chemical Co. Dopamine hydrochloride was purchased from Yuancheng Technology Development Co. Ltd. (China). *N*-hydroxysuccinimide (NHS) and 1-ethyl-3-[3-dimethylaminopropyl] carbodiimide hydrochloride (EDC) were purchased from Shanghai Medpep Co. Ltd. (China). Sodium dihydrogen phosphate dehydrate, sodium phosphate dibasic dodecahydrate and, ethylenediaminetetra acetic acid disodium (EDTA) were purchased from Tianjin Guangfu Fine Chemical Research Institute (China). The purified water was obtained with the Millipore Milli-Q purification system before use. Fluorescent-labeled enzymes were prepared as follows: mixtures of enzyme and FITC were incubated overnight under ambient conditions (50 mM phosphate buffer, pH 8.0, enzyme concentration 1 mg mL^{-1}, [dye]/[enzyme] = 5), followed by dialysis with a MW cutoff of 14 000 against PBS (50 mM, pH 7.0) for 72 h and water for another 24 h.

2.2. Methods. *2.2.1. Synthesis of Catechol-Modified Gelatin (GelC).* GelC was synthesized using EDC/NHS according to the standard amine coupling protocol. Dopamine was used as the source of catechol groups. Four grams of gelatin (4 mmol of carboxyl groups for type B) was dissolved in 100 mL PBS (50 mM, pH 5.5) at 40 °C. EDC (772.8 mg, 4 mmol), NHS (461.0 mg, 4 mmol), and the prescribed amount of dopamine (2−12 mmol) were added to the gelatin solution, and the reaction was conducted under N_2 protection at 40 °C for 12 h. The product was precipitated with cold alcohol (4 °C) three times followed by lyophilization. Catechol-modified gelatin (GelC) with different graft ratios were obtained by varying the molar ratio of amine groups from dopamine to carboxyl groups from gelatin (n = 1.0, 2.0, and 3.0) and denoted as $GelC_{1.0}$, $GelC_{2.0}$, and $GelC_{3.0}$, respectively.

2.2.2. Quantification of Free Amine Groups in Gelatin and GelC. The content of free amine groups in gelatin sample was determined by spectrophotometry using TNBS.[39,40] Five milligrams of gelatin sample was weighed into a test tube. One milliliter of 4% w/v sodium hydrogen carbonate ($NaHCO_3$, pH 8.5) and 1 mL of 0.5% w/v TNBS solution were added. The mixture was then heated at 40 °C for 2 h. The solution was further treated with 2 mL of 6 N HCl at 60 °C for 1.5 h. The absorbance of the solutions was determined at 350 nm after diluting 20 times. The percentage change of free amine groups was calculated using eq 1:

$$\text{Percentage change}(\%) = (A_{\text{GelC}}/A_{\text{Gel}} - 1) \times 100 \quad (1)$$

where A_{GelC} and A_{Gel} represented the absorbance of catechol-modified gelatin and native gelatin solutions, respectively.

2.2.3. Preparation of the GelCSi Hybrid Microcapsules. PAH (1.5 mg) was dissolved in $CaCl_2$ aqueous solution (1.5 mL, 0.33 M), then Na_2CO_3 solution (1.5 mL, 0.33 M) was rapidly added and continuously stirred for 30 s under ambient conditions. After the samples were allowed to settle for another 20 min, the PAH-doped $CaCO_3$ particles were collected by centrifugation and washed three times. Then, the obtained particles were suspended in the GelC aqueous solution (5 mL, 15 mg mL^{-1}) for 20 min. After centrifugation and washing four times, the $CaCO_3$ particles coated with GelC layer were obtained. The obtained particles were then suspended in 5 mL of Na_2SiO_3 solution (50 mM, pH 7.0−8.0) for 20 min to obtain the silica layer, followed by centrifugation and washing twice. The GelC−silica hybrid microcapsules (GelCSi) were obtained after removing $CaCO_3$ by EDTA solution (25 mM, pH 5.8).

2.2.4. Construction of the GelCSi-Based Enzyme Cascade System. FateDH (1.0 mg) and PAH (1.5 mg) were dissolved in $CaCl_2$ solution (1.5 mL, 0.33 M), then Na_2CO_3 solution (1.5 mL, 0.33 M) was rapidly added and continuously stirred for 30 s under ambient conditions. Then, the FateDH-containing $CaCO_3$ particles were suspended in 5 mL of 15 mg mL^{-1} GelC solution for 20 min. After they were centrifuged and washed, the FateDH-containing $CaCO_3$ particles coated with the GelC layer were collected. Next, the particles were suspended in 1 mL of 1.0 mg mL^{-1} FaldDH solution for 2 h with continuous shaking under ambient conditions and then rinsed twice with

dx.doi.org/10.1021/cs401096c | ACS Catal. 2014, 4, 962−972

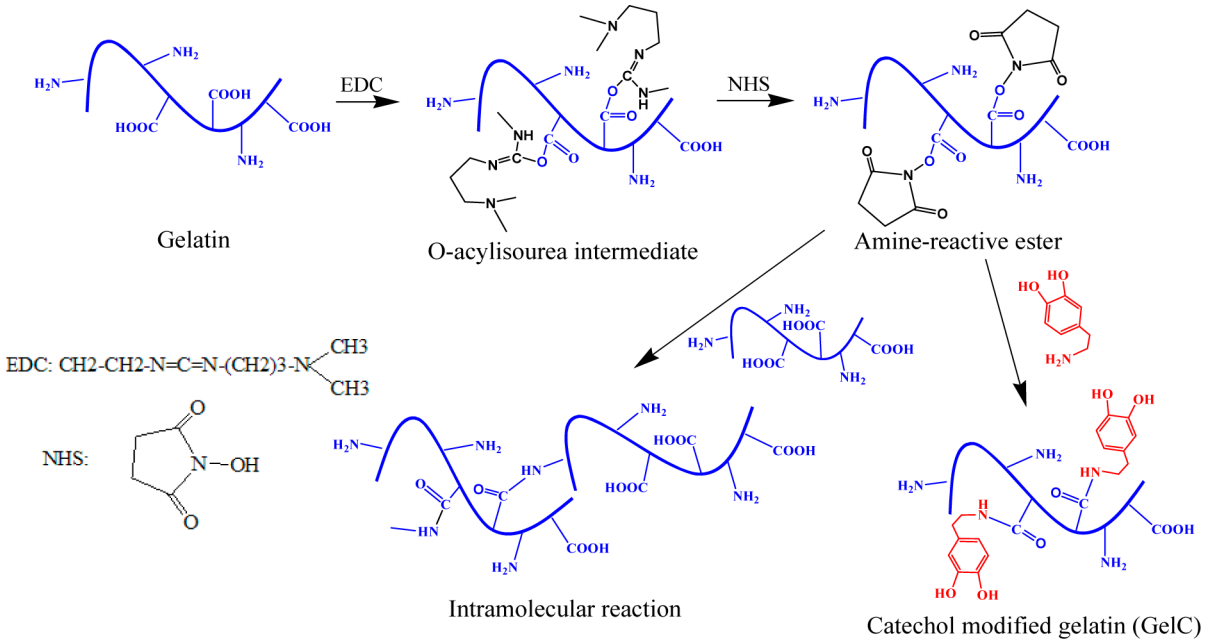

Figure 1. Schematic representation of the synthesis process of catechol-modified gelatin (GelC).

water to remove the residual FaldDH. The obtained particles were soaked in 5 mL of a 50 mM, pH 7.0−8.0 Na_2SiO_3 solution containing 1.0 mg of YADH for 20 min to obtain the silica layer. The GelCSi-based mutilenzyme cascade system was obtained after removal of the $CaCO_3$ cores by EDTA solution followed by three times of washing with PBS (50 mM, pH 7.0). The procedure for measuring the loading capacity of each enzyme can be found in the Supporting Information.

2.2.5. Enzymatic Conversion of Carbon Dioxide (CO_2) to Methanol. CO_2 was converted into methanol by conducting reduction reactions in aqueous solution with free or immobilized enzymes. The process encompassed three consecutive reduction steps: CO_2 to formic acid catalyzed by FateDH, formic acid to formaldehyde catalyzed by FaldDH, and formaldehyde to methanol catalyzed by YADH. NADH was used as a reducing agent to donate electrons for each reaction step. The experimental setup used in this study was described in detail in Scheme S1 of the Supporting Information. Conversion of CO_2 by the GelCSi-based enzyme cascade system was performed as follows. Briefly, immobilized-enzyme-containing solution (1 mL, 50 mM PBS, pH 7.0) was bubbled with CO_2 gas for 0.5 h, and then NADH solution (1 mL, 50 mM PBS, pH 7.0) was added to initiate the reaction. The operating pressure was maintained at 0.3 MPa by regulating the counterbalance valve. After the reaction, 20 uL of sample was taken from the reaction mixture after pressure release. The methanol concentration was analyzed by gas chromatography (Agilent 6820) with a thermal conductivity detector (TCD). All the measurements were repeated three times. The vaporization loss of methanol was not taken into account, and the concentrations of intermediate products, formic acid, and formaldehyde were too low to be detected. Moreover, 1 mol of methanol would consume 3 mols of NADH.[15,20]

The NADH conversion ratio (X_{NADH}, t), methanol yield ($Y_{methanol}$, t), methanol selectivity (S, %) and specific activity (ν_t, μmol min^{-1} mg^{-1}enzyme) were calculated according to eqs 2−5, respectively

$$X_{NADH,t}(\%) = \frac{C_{NADH,initial} - C_{NADH,t}}{C_{NADH,initial}} 100 \quad (2)$$

$$Y_{methanol,t} = \frac{3 \times C_{methanol,t}}{C_{NADH,initial}} 100 \quad (3)$$

$$S(\%) = \frac{Y_{methanol,t}}{X_{NADH,t}} 100 \quad (4)$$

$$\nu_t = \frac{V_{system}(C_{methanol,t-\Delta t} - C_{methanol,t})}{M_{enzyme}\Delta t} 100 \quad (5)$$

where $C_{NADH,initial}$ was the initial NADH concentration before the enzymatic reaction (μM), $C_{NADH,t}$ was the NADH concentration at the time of t (μM), $C_{methanol,t}$ was the methanol concentration at the time of t (μM), $C_{methanol,\ t-\Delta t}$ was the methanol concentration at the time of $t - \Delta t$ (μM), V_{system} was the solution volume of the system (L), and M_{enzyme} was the mass of enzymes used in the system (mg). The concentration of NADH throughout the experiments was diluted 200−400 times before determining at 340 nm by using the UV spectrophotometer.

2.2.6. Characterizations. The graft ratio of GelC was measured using a UV spectrometer (Hitachi U-3010, Japan). The chemical structure of GelC was characterized using ^{1}H NMR spectroscopy (AVANCE III 400M, Switzerland). The surface zeta-potentials of particles were measured in water with a Brookhaven zeta-potential analyzer. The measurements were repeated five times for each sample, and the average value was calculated. SEM images of the GelCSi microcapsules were recorded by using a field emission scanning electron microscope (FESEM, Nanosem 430). An energy dispersive spectroscope (EDS) attached to FESEM was used to analyze the elemental composition of microcapsules. TEM images of the GelCSi microcapsules were generated on a JEM-100CX II instrument. Thermogravimetric analysis (TGA) of the GelCSi microcapsules was performed on a Perkin-Elmer Pyris analyzer

dx.doi.org/10.1021/cs401096c | ACS Catal. 2014, 4, 962−972

under air atmosphere from 40 to 800 °C. The surface properties of the GelCSi microcapsules were analyzed by XPS in a Perkin−Elmer PHI 1600 ESCA system. Solid-state ^{29}Si MAS NMR spectra of the microcapsules shell were recorded on an Infinity Plus-300 MHz spectrometer, spin at 3 kHz. Nitrogen adsorption−desorption isotherm measurements were performed at 77 K on a Tristar 3000 gas adsorption analyzer to determine the pore-size distribution of the GelCSi microcapsules. Pore-size distribution curves were calculated using the Barrett−Joyner−Halenda (BJH) method. Confocal laser scanning microscopy (CLSM) images were taken with a Leica TCS SP5 microscope at the excitation wavelength of 488 nm according to the FITC-labeled enzyme.

3. RESULTS AND DISCUSSION

3.1. Synthesis and Characterization of Catechol-Modified Gelatin (GelC). Gelatin, type B (carboxyl groups: 1 mmol g^{-1}gelatin) has more free carboxyl groups than type A (carboxyl groups: 0.8 mmol g^{-1} gelatin). Consequently, type B gelatin was used to synthesize catechol-modified gelatin (GelC). Catechol groups were from dopamine. The carboxyl groups of gelatin were activated using EDC/NHS and then grafted with the amine groups of dopamine, as illustrated in Figure 1. Specifically, the carboxyl groups on gelatin reacted with EDC, forming an *O*-acylisourea intermediate. The *O*-acylisourea intermediate was converted into an amine-reactive ester by the addition of NHS. Then, the amine-reactive ester reacted with dopamine to form GelC. During the reaction, N_2 was used as inert gas to prevent the self-polymerization of dopamine. The GelC polymers were white solids and can dissolve in 40 °C hot water.

In addition to carboxyl groups, gelatin also possessed primary amine groups with which the amine-reactive ester could react, and consequently, intramolecular reaction of gelatin could occur. Therefore, an insoluble hydrogel was formed when excess gelatin reacted with dopamine (therefore, $GelC_{0.5}$ was not available). The TNBS reaction was adopted to quantify the primary amine groups of gelatin before and after modification.[39,40] The percentage change of free amine groups was calculated and listed in Table 1. As for $GelC_{1.0}$, ∼7.6% free amine groups of gelatin was reacted with carboxyl groups of gelatin. The intramolecular reaction can be ignored for $GelC_{2.0}$ and $GelC_{3.0}$, because dopamine was easier to react with the amine-reactive ester due to the smaller steric hindrance.

Table 1. Percentage Change of the Free Amine Groups

sample	abs at 350 nm	percentage change
gelatin	0.697	
$GelC_{0.5}$	n.a.	
$GelC_{1.0}$	0.644	−7.60%
$GelC_{2.0}$	0.702	+0.72%
$GelC_{3.0}$	0.709	+1.72%

UV−vis spectra of gelatin and $GelC_n$ (n = 1.0, 2.0, and 3.0) solution were monitored, as shown in Figure 2a. After dopamine grafting, the appearance of a new peak at 280 nm indicated the successful modification of gelatin with dopamine. It has been verified that the peak was due to the stretching of the catechol groups.[27,28,41] The peak was strengthened as the dopamine content increased, validating the synthesis of catechol-modified gelatin with varying graft ratio. Moreover, the concentration of the conjugated dopamine molecules was calculated from a calibration curve given by monitoring the absorbance of a known concentration of dopamine. Therefore, the graft ratio and catechol content in GelC could be calculated, as shown in Table 2. The graft ratio could reach 22.4% when the molar ratio of amine groups from dopamine to carboxyl groups from gelatin was 3.0. It suggested that approximately 22.4% of the carboxyl groups in the gelatin chain were modified with catechol groups, and the catechol content was 224 μmol per 1 g of GelC. This was in good agreement with recent results reported for polysaccharides or protein conjugated with phenol derivatives.[27,42,43] In spite of the increased amount of dopamine in the reaction, the graft ratio of $GelC_{2.0}$ was comparable with that of $GelC_{3.0}$. Therefore, $GelC_{2.0}$ was used to prepare the hybrid GelCSi microcapsules for constructing a multienzyme cascade system.

The chemical structure of GelC was characterized using ^1H NMR spectroscopy. $GelC_{2.0}$ (100 mg mL^{-1}) was dissolved in D_2O for the subsequent measurement, and the result is shown in Figure 2b. ^1H NMR data were the following: δ 4.7 (m, the protons of anomeric carbon of gelatin), δ 0.8−4.6 (m, alkyl protons of gelatin),[42] and δ 6.8−7.4 (m, aromatic protons of dopamine).[44−46] This result further demonstrated the successful synthesis of catechol-modified gelatin.

3.2. Fabrication and Characterization of the GelCSi Hybrid Microcapsules. Our approach to construct GelCSi microcapsules by combining the unique function of catechol groups and gelatin is shown in Figure 3. PAH-doped $CaCO_3$ particles were prepared and used as templates for the subsequent formation of microcapsule lumen. The obtained particles were suspended in GelC solution to acquire a GelC layer. Nonbound GelC was removed through three centrifugation/water rinsing/redispersion cycles. Then, the particles were exposed to sodium silicate solution, and GelC induced the condensation of sodium silicate to silica. After removal of $CaCO_3$ by EDTA solution, the GelCSi microcapsules were obtained.

The surface zeta-potential of PAH-doped $CaCO_3$ particles were conducted in aqueous solution in order to ascertain the deposition of GelC onto the $CaCO_3$ particles. After PAH doping, the $CaCO_3$ particles were positively charged (29.7 mV), which assured the deposition of the negatively charged GelC (gelatin, type B has a pI of 4.7−5.2, whereas the pH value in our study was 6.8). PAH was doped within the $CaCO_3$ particles, endowing the particles' surface with positive charge, because the zeta-potential of $CaCO_3$ particles was −28 mV in the absence of PAH.[47] The surface charge of the particles became negative (−19.8 mV) after deposition of the negatively charged GelC, indicating that the deposition of GelC was driven by electrostatic interactions and hydrogen bonds. Furthermore, it was demonstrated that a double thickness of film was obtained by the introduction of catechol groups due to hydrogen bond, and $\pi-\pi$ stacking occurred within adjacent catechol-modified polymers.[48] Therefore, in this study, the high GelC adsorption capacity was also achieved due to the presence of the catechol groups. After the fabrication of a silica shell onto the outer surface of the GelC/$CaCO_3$ microparticle via a biomimetic mineralization process, the zeta-potential decreased to −29.7 mV from −19.8 mV, suggesting that a negative silica shell has been coated as the outmost layer. This result was in good accordance with previous studies,[37,49−52] which showed that gelatin could induce a rapid condensation of sodium silicate to form a negatively charged silica coating layer under ambient temperature and neutral pH in aqueous solution.

dx.doi.org/10.1021/cs401096c | ACS Catal. 2014, 4, 962−972

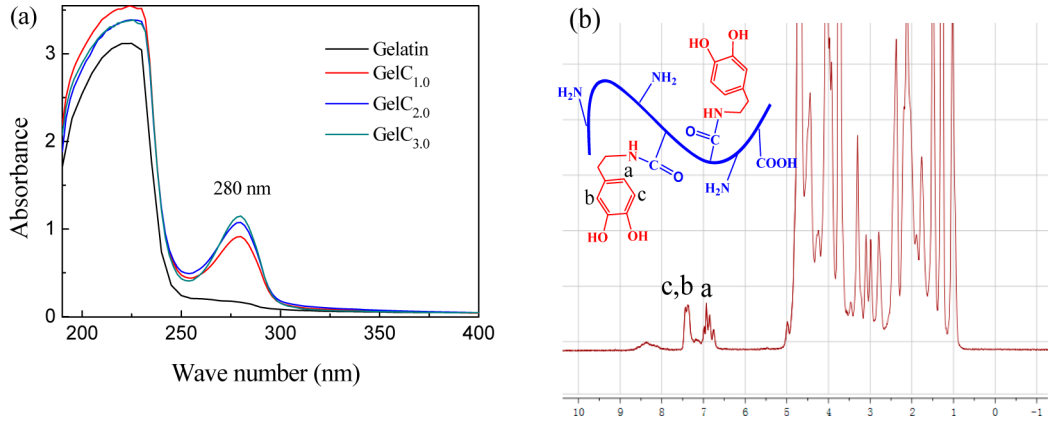

Figure 2. (a) UV−vis spectra of GelC aqueous solutions (2 mg mL^{-1}) and (b) ^1H NMR spectra of $GelC_{2.0}$.

Table 2. Graft Ratio and Catechol Content of GelC

sample	graft ratio	catechol content (μmol g^{-1} GelC)
$GelC_{0.5}$	n.a	n.a
$GelC_{1.0}$	17.2%	172
$GelC_{2.0}$	21.3%	213
$GelC_{3.0}$	22.4%	224

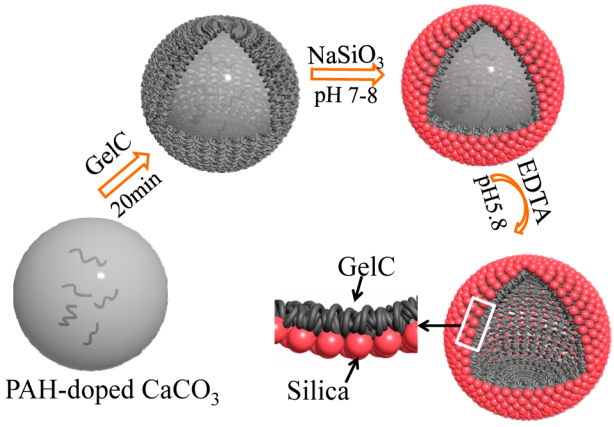

Figure 3. Preparation process of the GelCSi microcapsules.

The $CaCO_3$ core could be completely removed in EDTA, and the dissolution process was not hindered by the silica shell. SEM images revealed that the typical morphology of the microcapsules' folds and creases were due to interior water evaporation (Figure 4a,b). The GelCSi microcapsules had a diameter of ∼5 μm. Figure 4c indicated that the silica nanoparticles grew directly on the surface of the deposited GelC layer and revealed that a well-condensed silica shell was generated under the hydrolysis of GelC. The amine groups of gelatin chains acted as adsorption sites for silicates and induced their condensation; silica primary particles of 5−10 nm were obtained as a result of the growth of silicate nuclei.[41−43] TEM images (Figure 4d) revealed a very homogeneous surface, and no obvious aggregation of silica was observed in the shell of the GelCSi microcapsules. The shell was around 80 nm. AFM images (Figure 5a) further testified that uniform thickness of the microcapsules was obtained. From AFM height analysis (Figure 5b), the shell thickness of the capsules was determined to be half the minimum height of the collapsed flat regions (70 ± 5 nm), which was very close to the TEM analysis results. The aspect ratio between the diameter and the shell thickness was ∼71, indicating that the microcapsules possessed a very thin shell. It should be noted that, although the thickness of the shell

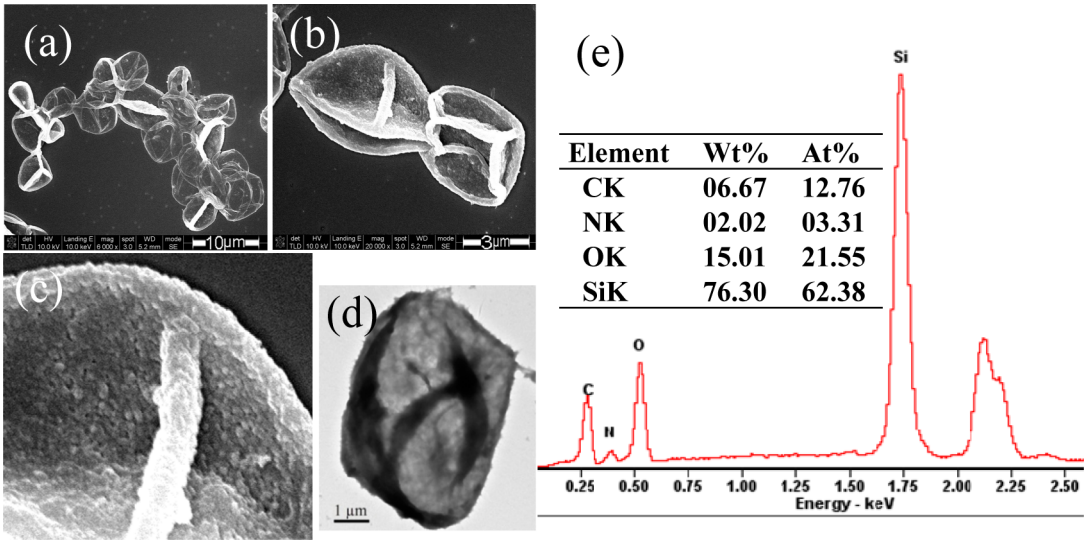

Figure 4. SEM images (a−c), TEM image (d), and EDX analysis (e) of the GelCSi microcapsules.

dx.doi.org/10.1021/cs401096c | ACS Catal. 2014, 4, 962−972

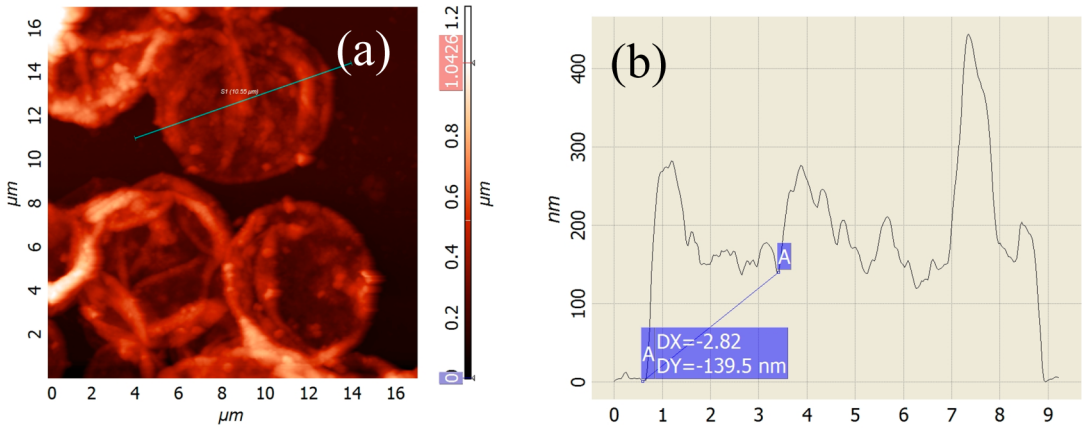

Figure 5. AFM image and shell thickness estimated from *z*-profile analysis of the GelCSi microcapsules.

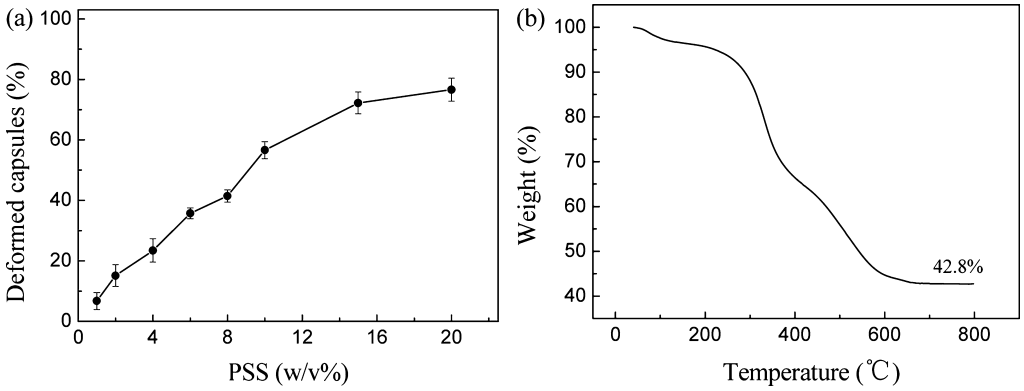

Figure 6. (a) Percentage of deformed microcapsules as a function of PSS concentration, (b) TGA curve of the GelCSi microcapsules.

was thin, no microcapsules were destroyed under the SEM and TEM measurement conditions.

The ultrathin shell of microcapsules with low mass transfer resistance was beneficial to effectively enhance the reaction efficiency. High stability was also of both scientific and technological importance. The method of penetrated pressure in different concentration of PSS solution can be used to assess the mechanical stability of microcapsules. The shrinking/buckling of microcapsules occurred when the elastic restoring force cannot compensate for the hydrostatic pressure difference, which developed from the concentration gradient of PSS. Hence, a shape transition of the microcapsules from spherical to cup shape would occur with increasing PSS concentration. The percentage of deformed microcapsule reflected the mechanical stability of microcapsules. As shown in Figure 6a, 56.6% of the GelCSi microcapsules were deformed in a 10 w/v % PSS solution, which was far lower than that of the polydopamine microcapsule,[34] PAH/PSS coacervation microcapsules,[53] and PGMA/PAH covalently attached microcapsules.[54] Thus, it was inferred that the hybrid microcapsules with an ultrathin shell exhibited a higher stability than organic capsules due to the introduction of a silica layer. A TGA curve (Figure 6b) showed that the mass fraction of the inorganic component in the GelCSi microcapsules was higher than 40%, and silica still dispersed homogeneously in the shell. Simultaneously, the introduction of gelatin enhanced flexibility of the microcapsules, because silica itself was quite brittle.[49]

Energy dispersive spectroscopy (EDS) analysis of the GelCSi microcapsules indicated that silicon was the primary component of the shell (Figure 4e). To confirm the presence of silica formed by in situ precipitation, X-ray photoelectron spectroscopy (XPS) and solid-state NMR spectroscopy were employed to investigate the condensation degrees. As shown in Figure 7a, there existed C, O, Si, and N elements in the XPS spectrum. C, N, and some O elements should be originated from GelC occluded in the microcapsules, and Si and some O elements should be originated from the silica layer. Moreover, the peak of Si2p at 103.0 and 102.0 eV corresponded to SiO_2 and SiOH[55−59] with relative percentages of 68.4% and 31.6%, respectively, in the high-resolution Si 2p XPS spectrum (Figure 7b). The ^{29}Si NMR spectrum (Figure 7c) revealed two major peaks at a chemical shift of −101.6 and −110.3 ppm, which were attributed to Q^3 [$Si(OSi)_3(OH)$] and Q^4 [$Si(OSi)_4$] with relative percentages of 28.3% and 71.7%, respectively. The percentage of SiO_2 was close to that obtained by XPS. The high content of Q^4 up to 71.7% indicated a fairly high proportion of condensed silanols in the shell of the microcapsules. It was suggested that GelC was a good inducer to hydrolyze sodium silicate to silica.

The pore size distribution of the GelCSi microcapsules was determined by the BET analysis. The nitrogen adsorption isotherms of the GelCSi microcapsules (Figure 7d) showed type IV isotherm characteristic of mesoporous materials, according to the IUPAC nomenclature. A pore size distribution curve was plotted based on the nitrogen adsorption−desorption isotherms, which revealed that the pore diameter of the GelCSi microcapsules was around 3.6 nm. This pore diameter allowed substrates and products (hydrodynamic diameter of all these molecules were less than 1 nm) to enter and leave the microcapsules lumen freely, whereas the majority

dx.doi.org/10.1021/cs401096c | *ACS Catal.* 2014, 4, 962−972

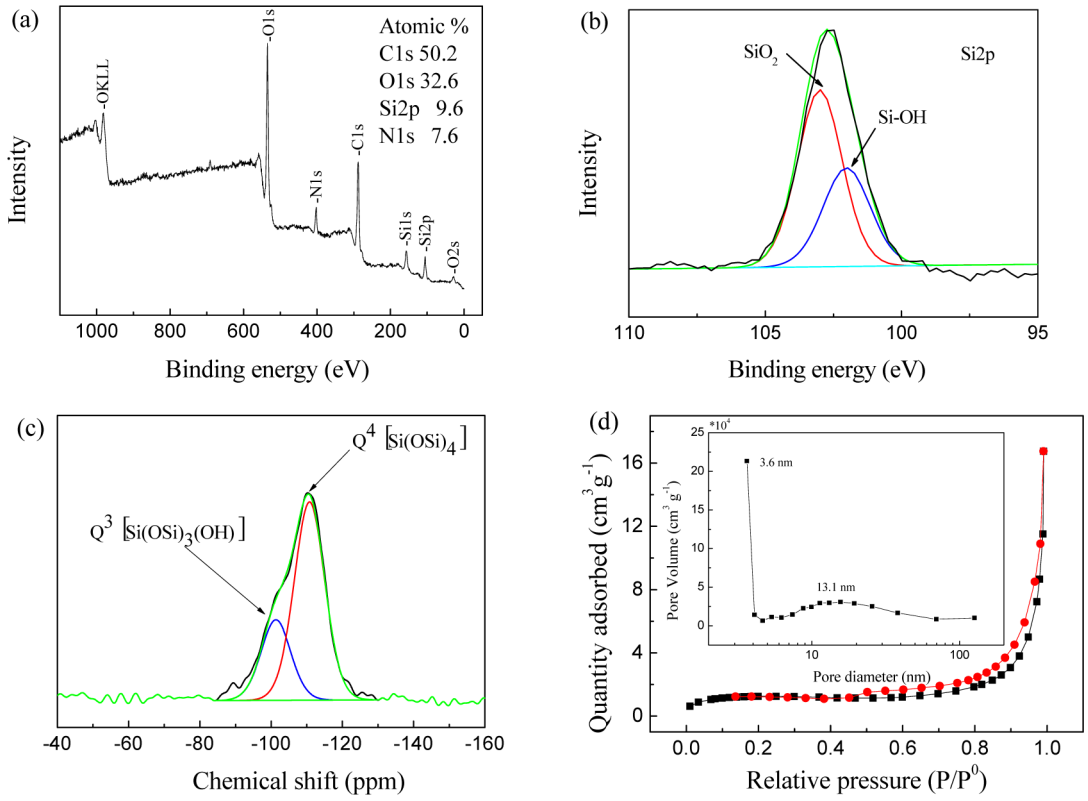

Figure 7. (a) XPS spectrum, (b) the high-resolution Si 2p spectrum, (c) ^{29}Si NMR spectrum, and (d) the nitrogen adsorption−desorption isotherms (inset was the pore size distribution curve by the BJH method) of the GelCSi microcapsules.

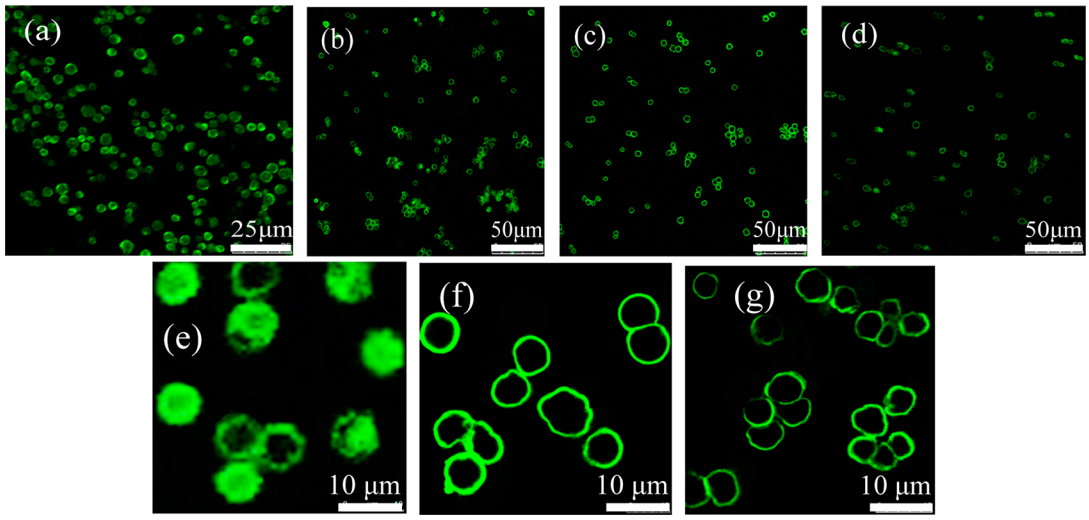

Figure 8. CLSM images of FateDH-containing $CaCO_3$ particles (a) and the GelCSi microcapsules with FateDH encapsulated in the microcapsules lumen (b, e), FaldDH covalently attached onto the GelC layer (c, f), and YADH entrapped in the silica layer (d, g).

of enzyme molecules were retained, because their hydrodynamic diameters were ∼7−10 nm. It was demonstrated that the mesoporous silica support played an important role in enhancement of the catalytic activities.[60] The mesoporosity of the microcapsule shell was due to the texture porosity formed by nanoparticle aggregation, which resulted from the interspace among nanoparticles.[37,38,49] It has been demonstrated that silica growth via the surface or solution mechanism did not significantly influence the silica structure.[61] Therefore, rapid growth of the silica nanoparticles took place on the outer surface of the GelC layer, causing disperse pore size formation due to time constraints and forming the mesoporous shell of the microcapsules.

3.3. Catalytic Efficiency and Stabilities of the Enzyme Cascade System. CO_2 was converted to methanol by successively catalysis with three types of enzyme under mild conditions.[15] The conversion comprised the initial reduction of CO_2 to formic acid catalyzed by FateDH and the reduction of formic acid to formaldehyde catalyzed by FaldDH. Finally, the formaldehyde was reduced to methanol by YADH. NADH acted as a reducing agent to donate electrons for each step.

dx.doi.org/10.1021/cs401096c | ACS Catal. 2014, 4, 962−972

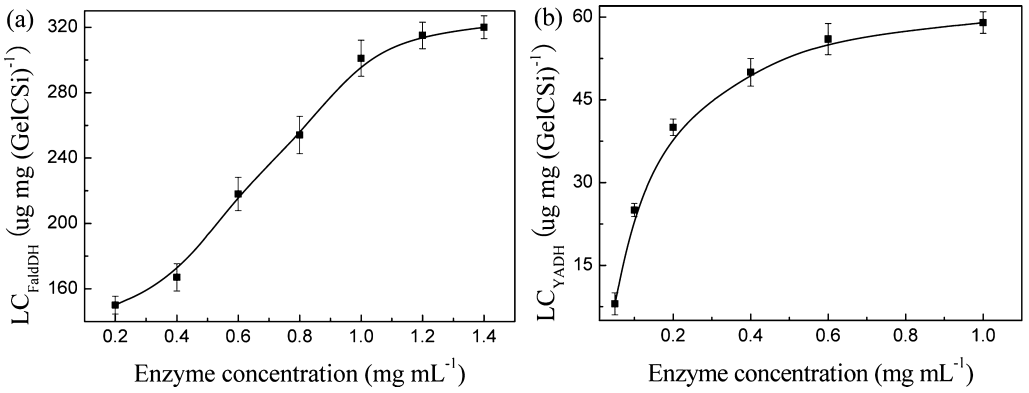

Figure 9. Loading capacities of (a) FaldDH in the GelC layer and (b) YADH in the silica layer as a function of enzyme concentration.

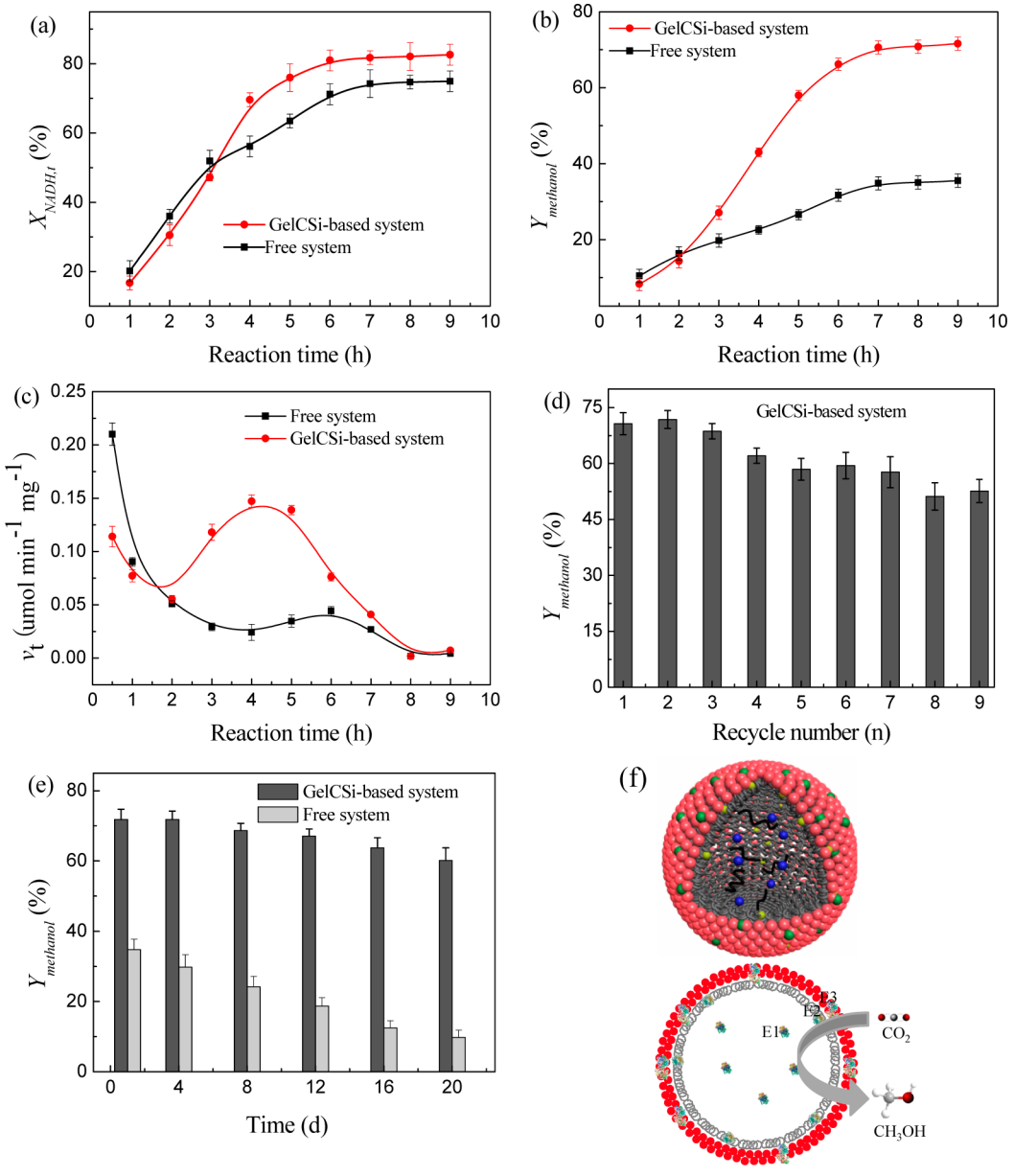

Figure 10. Plots of (a) NADH conversion ratio, (b) methanol yield, and (c) specific activity as a function of reaction time for converting CO_2 to methanol of the free and GelCSi-based enzyme cascade systems. (d) Recycling stability and (e) storage stability (the reaction was carried out for 6 h at 37 °C and pH 7.0). (f) Proposed reaction process of CO_2 to methanol catalyzed by the GelCSi-based system.

dx.doi.org/10.1021/cs401096c | ACS Catal. 2014, 4, 962−972

Confocal laser scanning microscope (CLSM) was employed to confirm the locations of the three enzymes. The relevant enzyme immobilization mechanism can be proposed. Each enzyme was labeled by FITC and separately immobilized in the microcapsules in the absence of the other two enzymes. Because FateDH (the first enzyme) was captured by $CaCO_3$ templates in the coprecipitation process for their formation and physically encapsulated in the lumen of the GelCSi microcapsules, the fluorescence signal on the $CaCO_3$ templates validated that the FITC-labeled FateDH was found throughout the particles and dispersed in the particles (Figure 8a). The microcapsules were prepared with these $CaCO_3$ templates, and the fluorescence signal (Figure 8b,e) revealed that the FITC-labeled FateDH was immobilized in the lumen of microcapsules. FateDH loading capacity in the lumen was about 300 μg mg (GelCSi)$^{-1}$. The second enzyme, FaldDH, was covalently attached with GelC via Michael addition and Schiff base reactions between amine groups of FaldDH and catechol groups of GelC. As expected, FaldDH was homogeneously dispersed within the shell of the microcapsule, and no FaldDH existed in the microcapsule lumen, as shown in Figure 8c,f. FaldDH loading capacity depended upon the enzyme concentration, increased quickly, and afterward remained nearly constant (Figure 9a). The loading capacity of individual enzyme was regulated according to the catalytic activity of each enzyme. FaldDH (1−6 U mg^{-1} enzyme) has a comparable activity with FateDH (5−15 U mg^{-1} enzyme); consequently, their loading capacity should be approximately the same. The loading capacity of FaldDH was 300 μg mg (GelCSi)$^{-1}$ as the concentration reached 1.0 mg mL^{-1}. GelC induced the hydrolysis and condensation of silicate, and YADH (the third enzyme) was entrapped accompanying the formation of the silica particles.[18,35] As a result, YADH was also uniformly distributed within the shell of the microcapsule (Figure 8d,g). The loading capacity of YADH (300 U mg^{-1} enzyme) should be approximately a tenth of that of FateDH and FaldDH according to the enzyme activity. When the concentration reached 0.2 mg mL^{-1}, 40 μg mg (GelCSi)$^{-1}$ of YADH could be immobilized in the silica layer (Figure 9b). The fluorescence signal (Figure 8d,g) was relatively weak, because the amount of immobilized FITC-labeled YADH was lower than that of the other two enzymes. The CLSM images showed that the microcapsules had a hollow shell structure about 5 μm in size, in good agreement with the SEM and TEM results (Figure 4a−d). All the above results implied that the three enzymes were successfully immobilized by the GelCSi microcapsules. The GelCSi microcapsules enabled the precise placement of components of enzymatic cascades within nanometer distances and the flexible regulation of the amount of individual enzyme according to each enzyme activity.

The methanol yield (Y, %) calculations were performed on the basis of the fact that 1 mol of methanol consumed 3 mols of NADH. Batch reactions were operated with the immobilized enzymes (FateDH, 0.30 mg; FaldDH, 0.30 mg; YADH, 0.04 mg), and the concentration of NADH was fixed at 50 mM. By contrast, the reactions were also carried out with the catalysis of free enzyme (FateDH, 0.30 mg; FaldDH, 0.30 mg; YADH, 0.04 mg).

The methanol yield and NADH conversion ratio of the free and GelCSi-based enzyme cascade system were investigated under optimal conditions (37 °C and pH 7.0). As illustrated in Figure 10a, the GelCSi-based system exhibited a NADH conversion ratio of 82.6%, which was higher than that of the free enzyme system (75.0%). The methanol yields increased, but afterward, they retained a constant value as the reaction time prolonged during the 9 h reaction for both systems (Figure 10b). Specifically, the methanol yield of the GelCSi-based systems was higher than that of the free system throughout the reaction process. The GelCSi-based systems exhibited a methanol yield of 71.6% after reaction equilibrium, which was much higher than that of the free system (35.5%). This result was attributed to the fact that the enzymes were specifically assembled within nanometer distances, which facilitated the direct transfer of an intermediate between consecutive enzymes without equilibrating with the bulk fluid. Although the free system exhibited higher activity in the early stages of the reaction, the reaction rate quickly decreased to zero due to the existence of reaction equilibrium (Figure 10c). The methanol selectivity of the GelCSi-based system was 86.7% as the reaction reached equilibrium, which was significantly higher than that of free enzyme system (47.3%), suggesting that the equilibrium was shifted substantially toward the products. This enhanced productivity of the GelCSi-based systems would lead to improved technological competitiveness. It should be noted that the methanol selectivity cannot be 100%, because the intermediates (formic acid and formaldehyde) cannot completely convert to methanol due to the reaction equilibrium.

The equilibrium shift in the GelCSi-based systems could be ascribed to the following aspects. As shown in Figure 10f, CO_2 was first transferred through the shell of the microcapsules into the microcapsule lumen to contact with FateDH and was converted to formic acid. Subsequently, formic acid went through the GelC layer to escape, fully contacted with FaldDH wherein, and was converted into formaldehyde. Similarly, formaldehyde contacted YADH and was converted into methanol, when it escaped from the silica layer. As a result, the diffusion distance for the reaction intermediates (formic acid and formaldehyde) to travel was decreased to nanometers between the active sites of FateDH, FaldDH, and YADH.[20,62,63] However, for the free enzyme system, the intermediates (formic acid and formaldehyde) have to diffuse through a longer distance to interact with FaldDH (YADH) before the formation of formaldehyde (methanol); therefore, the concentration of CO_2, formic acid, and formaldehyde were low and homogeneous.[15,16] In contrast, an assembly line was constructed by using the GelCSi hybrid microcapsules, and this process increased the throughput of the enzyme cascade system.[63,64]

Meanwhile, the methanol yield with recycling times of the GelCSi-based system was evaluated. As shown in Figure 10d, the methanol yield was continuously decreased as the recycling times increased for the GelCSi-based system. This decrease of methanol yield primarily resulted from the mass loss of the microcapsules after each reaction batch.[19] After nine cycles, the methanol yield decreased from 71.0% to 52.6%, and only 37.0% of the GelCSi microcapsules were left over. Moreover, the effect of storage on the methanol yields were examined (Figure 10e). In comparison to the free enzyme system, the GelCSi-based system showed high enzyme activity retention and significant enzyme stability during storage. This result was probably the result of the following: (1) the interaction between the three enzymes was reduced or avoided by separated immobilization of each enzyme;[65] (2) enzyme molecules with a size of about 7 nm were unable to leak out of the GelCSi microcapsules during the storage process,

dx.doi.org/10.1021/cs401096c | ACS Catal. 2014, 4, 962−972

because the pore size of the GelCSi microcapsules was about 3.6 nm.

4. CONCLUSIONS

With the coupling of two platform technologies—biomimetic mineralization and bioadhesion—a multienzyme cascade system using hybrid microcapsules as a scaffold was constructed for efficient conversion of CO_2 to methanol. The GelCSi hybrid microcapsules were prepared through the deposition of catechol-modified gelatin (GelC) followed by in situ growth of silica nanoparticles on the GelC layer. Three enzymes, formate dehydrogenase, formaldehyde dehydrogenase, and alcohol dehydrogenase, were, respectively, immobilized through physical entrapment in the capsule lumen, covalent attachment onto the GelC layer, and physical entrapment in the silica layer. The GelCSi microcapsules enabled the precise placement of substrates/intermediates of enzymatic cascades within nanometer distances and the rational regulation of the amount of individual enzyme according to each enzyme activity. The microcapsules possessed ultrathin, mesoporous shell (thickness: 70 nm, pore size: 3.6 nm), which endowed the rapid mass transfer. The yield and selectivity of the GelCSi-based system (71.6%, 86.7%) were remarkably higher than those of the free enzyme system (35.5%, 47.3%). Moreover, the GelCSi microcapsules displayed high mechanical stability, which provided the GelCSi-based system with good recyclability and an appropriate microenvironment for storage stability. Hopefully, the approach developed in this study will be useful for constructing high-efficiency catalytic systems for various enzymatic/chemical conversions.

■ ASSOCIATED CONTENT

Supporting Information

Supplementary data as noted in the text. This material is available free of charge via the Internet at http://pubs.acs.org.

■ AUTHOR INFORMATION

Corresponding Author

*E-mail: zhyjiang@tju.edu.cn.

Notes

The authors declare no competing financial interest.

■ ACKNOWLEDGMENTS

The authors are thankful for financial support from the National Science Fund for Distinguished Young Scholars (21125627), the National Basic Research Program of China (2009CB724705), the National Science Foundation of China (20976127, 21076145), and the Program of Introducing Talents of Discipline to Universities (B06006).

■ REFERENCES

(1) Mikkelsen, M.; Jørgensen, M.; Krebs, F. C. *Energy Environ. Sci.* **2010**, *3*, 43−81.
(2) Yang, H.; Xu, Z.; Fan, M.; Gupta, R.; Slimane, R. B.; Bland, A. E.; Wright, I. *J. Environ. Sci.* **2008**, *20*, 14−27.
(3) Appel, A. M.; Bercaw, J. E.; Bocarsly, A. B.; Dobbek, H.; DuBois, D. L.; Dupuis, M.; Ferry, J. G.; Fujita, E.; Hille, R.; Kenis, P. J. *Chem. Rev.* **2013**, *133*, 6621−6658.
(4) Hawkins, A. S.; McTernan, P. M.; Lian, H.; Kelly, R. M.; Adams, M. W. *Curr. Opin. Biotechnol.* **2013**, *24*, 376−384.
(5) Qiao, J.; Liu, Y.; Hong, F.; Zhang, J. *Chem. Soc. Rev.* **2014**, *43*, 631−675.
(6) Forsyth, C.; Yip, T. W. S.; Patwardhan, S. V. *Chem. Commun.* **2013**, *49*, 3191−3193.
(7) Glueck, S. M.; Gümüs, S.; Fabian, W. M. F.; Faber, K. *Chem. Soc. Rev.* **2009**, *39*, 313−328.
(8) Baskaya, F. S.; Zhao, X.; Flickinger, M. C.; Wang, P. *Appl. Biochem. Biotechnol.* **2010**, *162*, 391−398.
(9) Zhao, H. *ACS Catal.* **2011**, *1*, 1119−1120.
(10) Santacoloma, P. A.; Sin, G. r.; Gernaey, K. V.; Woodley, J. M. *Org. Process Res. Dev.* **2010**, *15*, 203−212.
(11) Schoffelen, S.; van Hest, J. C. M. *Soft Matter* **2012**, *8*, 1736−1746.
(12) Tran, D. N.; Balkus, K. J. *ACS Catal.* **2011**, *1*, 956−968.
(13) Sheldon, R. A.; van Pelt, S. *Chem. Soc. Rev.* **2013**, *42*, 6223−6235.
(14) Sheldon, R. A. *Chem. Soc. Rev.* **2012**, *41*, 1437−1451.
(15) Obert, R.; Dave, B. C. *J. Am. Chem. Soc.* **1999**, *121*, 12192−12193.
(16) El-Zahab, B.; Donnelly, D.; Wang, P. *Biotechnol. Bioeng.* **2008**, *99*, 508−514.
(17) Shi, J.; Wang, X.; Jiang, Z.; Liang, Y.; Zhu, Y.; Zhang, C. *Bioresour. Technol.* **2012**, *118*, 359−366.
(18) Shi, J.; Zhang, L.; Jiang, Z. *ACS Appl. Mater. Interfaces* **2011**, *3*, 881−889.
(19) Shi, J.; Wang, X.; Zhang, W.; Jiang, Z.; Liang, Y.; Zhu, Y.; Zhang, C. *Adv. Funct. Mater.* **2013**, *23*, 1450−1458.
(20) Jiang, Y.; Sun, Q.; Zhang, L.; Jiang, Z. *J. Mater. Chem.* **2009**, *19*, 9068−9074.
(21) Sun, Q. Y.; Jiang, Y. J.; Jiang, Z. Y.; Zhang, L.; Sun, X. H.; Li, J. *Ind. Eng. Chem. Res.* **2009**, *48*, 4210−4215.
(22) Lee, H.; Dellatore, S.; Miller, W.; Messersmith, P. *Science* **2007**, *318*, 426−430.
(23) Ryou, M.-H.; Kim, J.; Lee, I.; Kim, S.; Jeong, Y. K.; Hong, S.; Ryu, J. H.; Kim, T.-S.; Park, J.-K.; Lee, H.; Choi, J. W. *Adv. Mater.* **2012**, *25*, 1571−1576.
(24) Zeng, H.; Hwang, D.; Israelachvili, J.; Waite, J. *Proc. Natl. Acad. Sci. U.S.A. Early Ed.* **2010**, *107*, 12850−12854.
(25) Harrington, M.; Masic, A.; Holten-Andersen, N.; Waite, J.; Fratzl, P. *Science* **2010**, *328*, 216−220.
(26) Wang, X.; Jiang, Z.; Shi, J.; Liang, Y.; Zhang, C.; Wu, H. *ACS Appl. Mater. Interfaces* **2012**, *4*, 3476−3483.
(27) Ryu, J. H.; Lee, Y.; Kong, W. H.; Kim, T. G.; Park, T. G.; Lee, H. *Biomacromolecules* **2011**, *12*, 2653−2659.
(28) Lee, Y.; Chung, H. J.; Yeo, S.; Ahn, C. H.; Lee, H.; Messersmith, P. B.; Park, T. G. *Soft Matter* **2010**, *6*, 977−983.
(29) Kim, K.; Ryu, J. H.; Lee, D. Y.; Lee, H. *Biomater. Sci.* **2013**, *1*, 783−790.
(30) Zvarec, O.; Purushotham, S.; Masic, A.; Ramanujan, R. V.; Miserez, A. *Langmuir* **2013**, *29*, 10899−10906.
(31) Cho, J. H.; Shanmuganathan, K.; Ellison, C. J. *ACS Appl. Mater. Interfaces* **2013**, *5*, 3794−3802.
(32) Bittner, S. *Amino Acids* **2006**, *30*, 205−224.
(33) Lee, H.; Rho, J.; Messersmith, P. B. *Adv. Mater.* **2009**, *21*, 431−434.
(34) Zhang, L.; Shi, J.; Jiang, Z.; Jiang, Y.; Qiao, S.; Li, J.; Wang, R.; Meng, R.; Zhu, Y.; Zheng, Y. *Green Chem.* **2011**, *13*, 300−306.
(35) Zhang, L.; Shi, J.; Jiang, Z.; Jiang, Y.; Meng, R.; Zhu, Y.; Liang, Y.; Zheng, Y. *ACS Appl. Mater. Interfaces* **2011**, *3*, 597−605.
(36) Cui, J.; Yan, Y.; Such, G. K.; Liang, K.; Ochs, C. J.; Postma, A.; Caruso, F. *Biomacromolecules* **2012**, *13*, 2225−2228.
(37) Yang, X.; Liao, S.-J.; Liang, Z.-X.; Li, Y.-X.; Du, L. *Microporous Mesoporous Mater.* **2011**, *143*, 263−269.
(38) Allouche, J.; Boissière, M.; Hélary, C.; Livage, J.; Coradin, T. *J. Mater. Chem.* **2006**, *16*, 3120−3125.
(39) Li, W.-M.; Liu, D.-M.; Chen, S.-Y. *J. Mater. Chem.* **2011**, *21*, 12381−12388.
(40) Won, Y.-W.; Kim, Y.-H. *J. Controlled Release* **2008**, *127*, 154−161.
(41) Lee, B. P.; Dalsin, J. L.; Messersmith, P. B. *Biomacromolecules* **2002**, *3*, 1038−1047.

(42) Park, K. M.; Lee, Y.; Son, J. Y.; Oh, D. H.; Lee, J. S.; Park, K. D. *Biomacromolecules* **2012**, *13*, 604−611.
(43) Hong, S.; Yang, K.; Kang, B.; Lee, C.; Song, I. T.; Byun, E.; Park, K. I.; Cho, S.-W.; Lee, H. *Adv. Funct. Mater.* **2012**, *23*, 1774−1780.
(44) Mallakpour, S.; Zadehnazari, A. *J. Chem. Sci.* **2013**, *125*, 203−211.
(45) Ai, Y.; Wei, Y.; Nie, J.; Yang, D. *J. Photochem. Photobiol., B* **2013**, *120*, 183−190.
(46) Park, J. Y.; Kim, J. S.; Nam, Y. S. *Carbohydr. Polym.* **2013**, *97*, 753−757.
(47) Fakhrullin, R. F.; Minullina, R. T. *Langmuir* **2009**, *25*, 6617−6621.
(48) Min, Y.; Hammond, P. T. *Chem. Mater.* **2011**, *23*, 5349−5357.
(49) Mahony, O.; Tsigkou, O.; Ionescu, C.; Minelli, C.; Ling, L.; Hanly, R.; Smith, M. E.; Stevens, M. M.; Jones, J. R. *Adv. Funct. Mater.* **2010**, *20*, 3835−3845.
(50) Lei, B.; Shin, K.-H.; Noh, D.-Y.; Jo, I.-H.; Koh, Y.-H.; Choi, W.-Y.; Kim, H.-E. *J. Mater. Chem.* **2012**, *22*, 14133−14140.
(51) Setyawan, H.; Balgis, R. *Asia-Pac. J. Chem. Eng.* **2012**, *7*, 448−454.
(52) Ruiz-Hitzky, E.; Aranda, P.; Darder, M.; Ogawa, M. *Chem. Soc. Rev.* **2011**, *40*, 801−828.
(53) Wang, F.; Feng, J.; Tong, W.; Gao, C. *J. Mater. Chem.* **2007**, *17*, 670−676.
(54) Feng, Z.; Wang, Z.; Gao, C.; Shen, J. *Adv. Mater.* **2007**, *19*, 3687−3691.
(55) Yuan, M.-r.; Lu, J.-t.; Kong, G. *Surf. Coat. Technol.* **2010**, *204*, 1229−1235.
(56) Sawyer, R.; Nesbitt, H.; Secco, R. *J. Non-Cryst. Solids* **2012**, *358*, 290−302.
(57) Fujita, K.; Oya, A.; Benoit, R.; Beguin, F. *J. Mater. Sci.* **1996**, *31*, 4609−4615.
(58) McEleney, K.; Crudden, C. M.; Horton, J. H. *J. Phys. Chem. C* **2009**, *113*, 1901−1907.
(59) Klapiszewski, Ł.; Nowacka, M.; Milczarek, G.; Jesionowski, T. *Carbohydr. Polym.* **2013**, *94*, 345−355.
(60) Lin, Y.; Li, Z.; Chen, Z.; Ren, J.; Qu, X. *Biomaterials* **2013**, *34*, 2600−2610.
(61) van Bommel, K. J.; Shinkai, S. *Langmuir* **2002**, *18*, 4544−4548.
(62) Tong, X.; El-Zahab, B.; Zhao, X.; Liu, Y.; Wang, P. *Biotechnol. Bioeng.* **2011**, *108*, 465−469.
(63) Idan, O.; Hess, H. *ACS Nano* **2013**, *7*, 8658−8665.
(64) LeDuc, P. R.; Wong, M. S.; Ferreira, P. M.; Groff, R. E.; Haslinger, K.; Koonce, M. P.; Lee, W. Y.; Love, J. C.; McCammon, J. A.; Monteiro-Riviere, N. A. *Nat. Nanotechnol.* **2007**, *2*, 3−7.
(65) Huthmacher, C.; Gille, C.; Holzhütter, H.-G. *J. Theor. Biol.* **2008**, *252*, 456−464.